# Dense Granular Flow

Annette Zippelius

Institute for Theoretical Physics, University of Göttingen

May 2017

# Wealth of Applications

## technical

food processing

random close packing

Chaikin et al. 2004

## and in nature

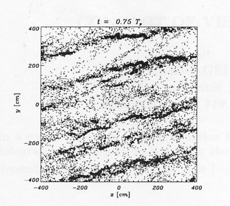


ring of Saturn

# ... of Fundamental Interest

**nonequilbrium** model system

- grain of sand of diameter $d$ at room temperature: $\frac{k_B T}{mgd} \sim 10^{-12}$
- interactions between macroscopic bodies are dissipative
- Grains left to themselves settle into static packing
- decay of an initially agitated state: cooling
- Dynamics due to driving, e.g. gravity, shear, fluidized beds,...

**rheology of dense granular matter**

How do these materials flow in response to an applied shear

# Rheology of dense granular matter

How do these materials flow in response to an applied shear?

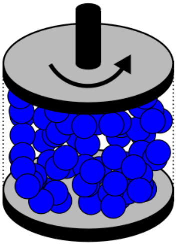

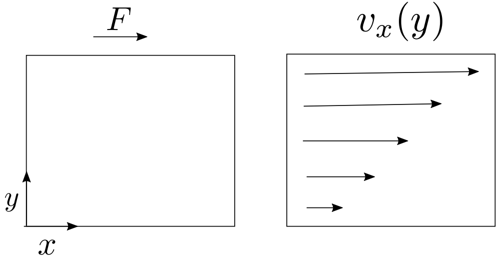


apply a stress (force/area) and measure the velocity or strain rate

$$\boxed{\dot{\gamma} = \partial_y v_x}$$

apply a velocity or displacement and measure the stress

# Rheology of dense granular matter

What is the relation between stress and strainrate?

$$\boxed{\sigma(\dot{\gamma}) = \eta(\dot{\gamma})\dot{\gamma}}$$

Newtonian fluid or colloidal suspension: $\eta(\dot{\gamma}) \to \dot{\gamma}$ as $\dot{\gamma} \to 0$
fluid of athermal, hard spheres (dry granular medium):

Bagnold scaling: $\boxed{\eta(\dot{\gamma}) \to \dot{\gamma} \qquad \sigma \propto \dot{\gamma}^2}$ as $\dot{\gamma} \to 0$

Large strainrates

shear thickening: $\eta(\dot{\gamma})$ increases with $\dot{\gamma}$

frictional granular fluid

shear thinning: $\eta(\dot{\gamma})$ decreases with $\dot{\gamma}$

frictionless granular fluid

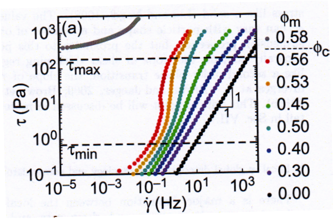


E. Brown and H. Jäger, Rep. Prog. Phys. **77**

# Frictionless Jamming

- jamming: a material becomes rigid with increasing packing fraction $\phi$
- control parameters for the fluid to solid transition:
  - shear stress $\sigma$
  - packing fraction $\phi$
- jamming transition is studied by monitoring flow curves

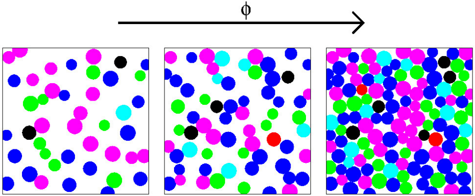


Frictionless spheres:

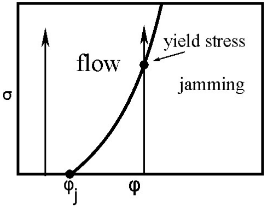


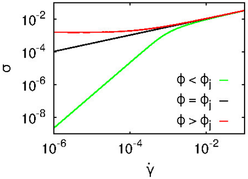

# Rheology of Frictional Grains

- Jamming of frictional particles

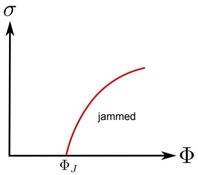


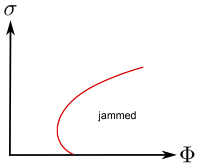


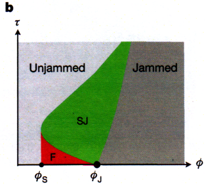


D. Bi et al., Nature **480** (2011)

phase diagram: first order phase transition and finite stress critical point in contrast to frictionless particles M. Grob, C. Heussinger and AZ, Phys. Rev. E **89**, 2014

- chaotic regime

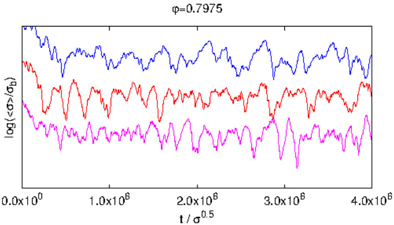


Rheo-Chaos

Aradian and Cates, Phys.Rev. E**73** (2005)

hydrodynamic model

M. Grob, AZ and C. Heussinger, Phys.Rev. E**93**, (2016)

# Grains with Friction

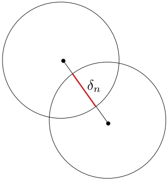


translational velocities $\mathbf{v}$ and rotational velocities $\boldsymbol{\omega}$

Newton's equations of motion

interactions only when the particles are in contact

model of soft spheres: normal and tangential forces

$$\boxed{F_n = -k_n \delta_n - \zeta_n v_n} \qquad \text{and} \qquad \boxed{F_t = -k_t \delta_t - \zeta_t v_t}$$

spring constants $k_n = k_t = 1$, damping constants $\zeta_n = \zeta_t = 1$

tangential overlap: $\delta_t = \int_{t_0}^{t} dt' v_t(t')$ as long as $\boxed{|F_t| < \mu |F_n|}$

$|F_t| = \mu |F_n| \rightarrow$ sliding contact; no loading of the tangential spring

Coulomb friction coefficient $\mu = 2 \rightarrow$ strong friction

polydisperse mixture

strain controlled simulations (Lees Edwards boundary conditions)

stress controlled simulations with rigid walls

critical discussion: S. Schäfer et al., J. Phys. **I6**, 5, 1996

# Deforming the System - Strain Controlled Simulation

impose strain rate $\dot{\gamma}$ and measure stress $\sigma$

different regimes:

- Bagnold: $\sigma \propto \dot{\gamma}^2$
- Plastic: $\sigma \propto \dot{\gamma}^{1/2}$
- $\phi > \phi_c$ stress jumps, hyteresis observable
- still larger $\phi$: finite yield stress

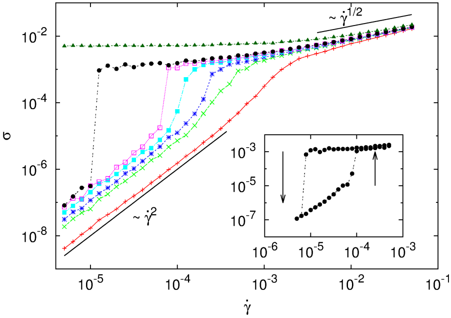


discontinuous transition;
hyteresis can be observed

# Proposing a Constitutive Relation - a Simple Model

- Bagnold: $\sigma \propto \dot{\gamma}^2 \Leftrightarrow \dot{\gamma} \propto \sigma^{1/2}$
- Plastic: $\sigma \propto \dot{\gamma}^{1/2} \Leftrightarrow \dot{\gamma} \propto \sigma^2$
- metastable: $\dot{\gamma}(\sigma)$ not monotonic

$$\boxed{\dot{\gamma}(\sigma) = a\sigma^{1/2} - b\sigma + c\sigma^2}$$

$a(\phi = \phi_\eta) = 0;\ b > 0, c > 0$ const.

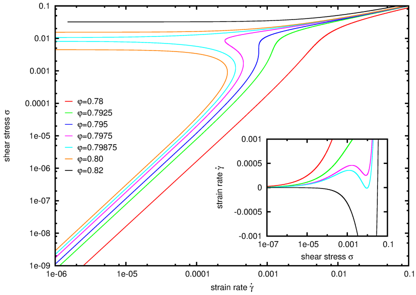


predictions:

- discontinuous transition with a critical point
- critical point $\phi_c$: vertical inflection point
- $\phi > \phi_c$: unstable region $\rightarrow$ stress jumps in the simulation
- $\phi = \phi_\sigma > \phi_c$: finite yield stress
- divergence of the viscosity at $\phi_\eta > \phi_\sigma > \phi_c$

# Phase Diagram I

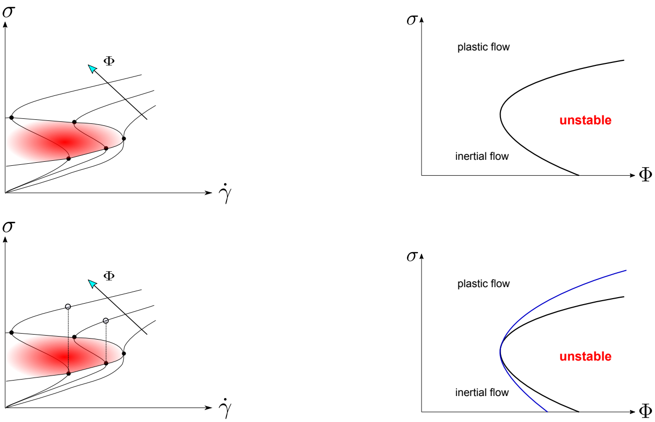


What happens in the unstable region? Phase separation?

# Phase Coexistence?

shear banding

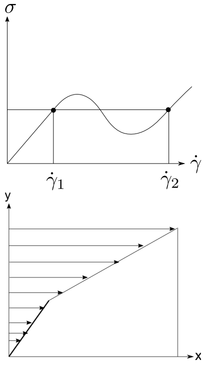


vorticity banding

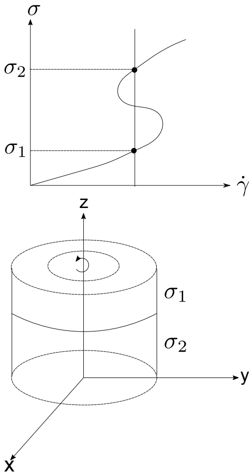


needs third dimension and pressure has to be balenced across the interface

# The Unstable Region - Stress Controlled Simulation

vary stress $\sigma_1 < \sigma_2 < \sigma_3 < \sigma_4 < \sigma_5$ at fixed $\phi$monitor $\dot{\gamma}_{\sigma_i}(t)$

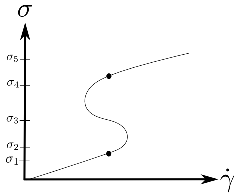


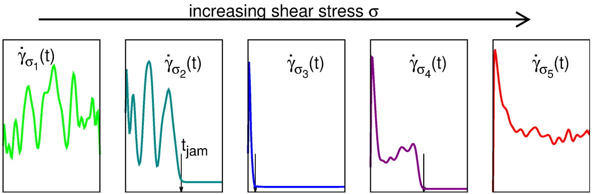


average over transient flow
S-shaped flow curve is observed
in transient behaviour

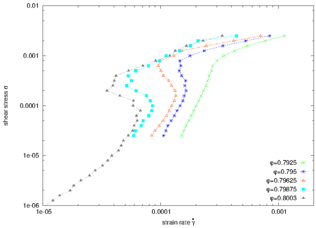

# Phase Diagram II

no shear or vorticity banding
shear controlled simulations
unstable region: jamming
metastable region: transient flow

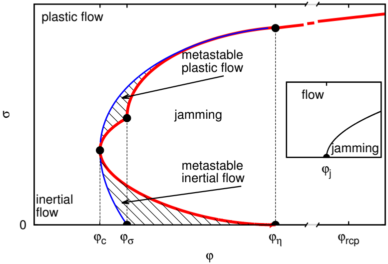


How can we understand reentrance?
reduce $\sigma$ $\rightarrow$ reduction in normal load
contacts which are blocked by the Coulomb criterion: $|F_t| < \mu|F_n|$
$|F_t| = \mu|F_n|$ become free to slide $\rightarrow$
grains can flow $\rightarrow$ unjamming
number of sliding contacts

Florian Spreckelse

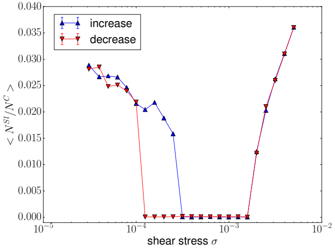

# Conclusion I

- re-entrant flow
- generic feature of friction
- non-zero stress critical point
- van-der-Waals-like phenomenology

$$\boxed{\dot{\gamma}(\sigma) = a\sigma^{1/2} - b\sigma + c\sigma^2}$$

- 3 critical densities (Otsuki and Hayakawa, PRE 2011)
- can reproduce all features of the phase diagram
- model includes ($b = 0$) the frictionless case $\mu = 0$

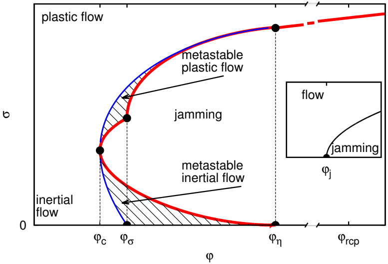


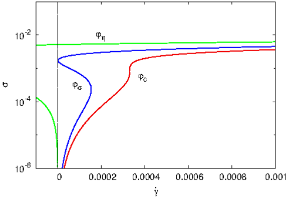


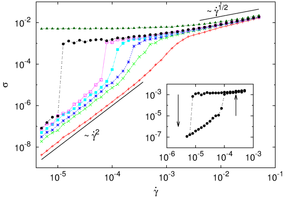

# Hydrodynamic Model

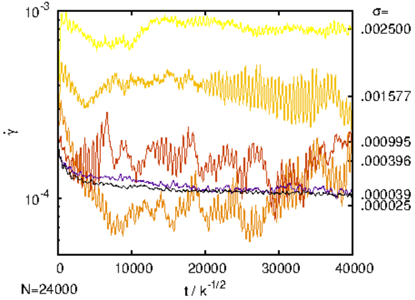


increase system size $\to$
no stationary solution
for a range of $\sigma$ and $\Phi$

momentum conservation

$$\partial_t v_x = \partial_y \sigma_{xy} \to \partial_t \dot\gamma = \partial_y^2 \sigma$$

microstructure characterized by scalar field $w(y,t)$;

- reduces strain rate as compared to the frictionless case:
  $\dot\gamma = \dot\gamma_0 - w; \quad \dot\gamma_0 = a\sqrt{\sigma} + c\sigma^2$
- relaxes to a stationary value: $\partial_t w = -(w - w^*)/\tau$
- stationary value $w^* = b\sigma; \quad 1/\tau \propto \dot\gamma$

Olmsted, Rheol. Acta **47**, 283 (2008); Nakanishi et al., PRE **85**, 011401 (2012)

# Hydrodynamic Model

$$\begin{aligned}\partial_t \dot\gamma &= \partial_y^2 \sigma \\ \dot\gamma &= \dot\gamma_0 - w \\ \partial_t w &= -\dot\gamma(w - w^*)\end{aligned}$$

stationary flow:

$\dot\gamma = a\sqrt{\sigma} - b\sigma + c\sigma^2,\ w = w^*,\ \sigma = \sigma_0$

jamming:

$\dot\gamma = 0,\ w = \dot\gamma_0,\ \sigma = \sigma_0$

linear stability analysis: $\delta\sigma, \delta w \sim e^{\Omega t} e^{iky}$

stationary flow is unstable: $\frac{\partial \dot\gamma}{\partial \sigma} < 0$

jammed state is stable for negative $\dot\gamma$

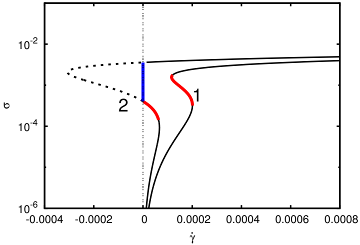

# Phase diagram III

predictions of the hydrodynamic model

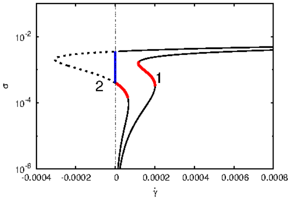


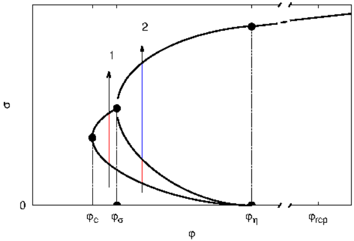


Simulations:

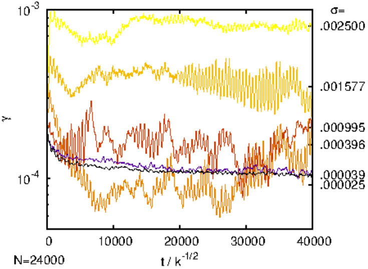


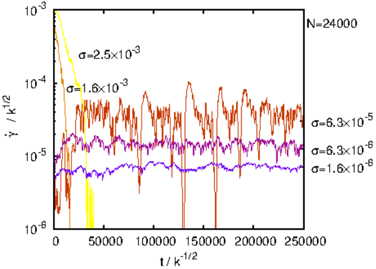

# How to characterize heterogeneous, chaotic states?

anisotropic and long ranged stress fluctuations in dilation direction

length scale $\sim$ system size

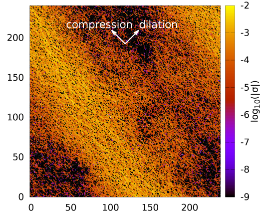


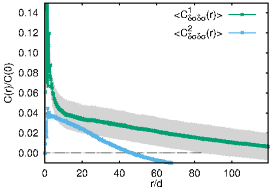


spectrum of strainrate fluctuations in stress controlled simulations

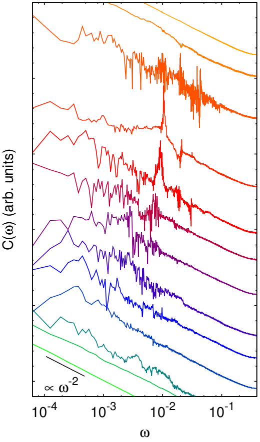


$$4 \times 10^{-7} \leq \sigma \leq 2,5 \times 10^{-2}$$

# Conclusions II

- re-entrant flow, nonzero stress critical point
- van der Waals like phenomenology
- spatio-temporal chaos besides stationary flow and jamming
- observable only for sufficiently large system size
- complex frequency dependent spectra and spatial correlations on scales of system size
- Hydrodynamic model: coupled dynamics of stress and microstructure
- stability analysis: time dependent states
- microstructure $\rightarrow \dot{\gamma}(\sigma) = a\sigma^{1/2} - b\sigma + c\sigma^2$

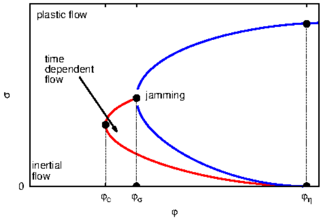


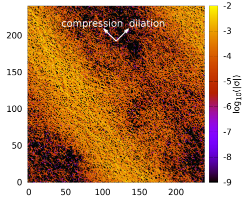

# Microscopic picture of friction induced shear thickening

## Shear Thickening: Ubiquitous Phenomenon

shear thickening observed in colloidal and non-Brownian suspensions

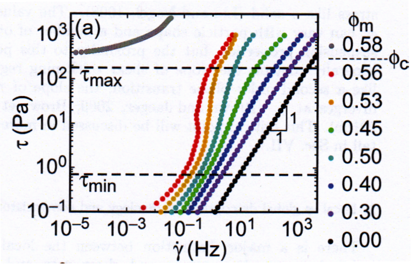


possible mechanisms:

- formation of hydroclusters
- shear induced glass transition
- viscosity of frictional system diverges at lower $\phi$; friction becomes effective for $f > f^*$ ; sharp crossover for $\sigma > \sigma^*$
- enforced flow $\rightarrow$ dilation; constant volume $\rightarrow$ large normal stresses $\rightarrow$ large shear resistance


E. Brown and H. Jäger, Rep. Prog. Phys. **77**, 2012; R. Seto et al. PRL **111**, 2013; C. Heussinger PRE **88**, 2013;

N. Fernandez et al. PRL **111**, 2013; Z. Pan et al. PRE **92**, 2014 ; E. DeGulie et al. arXiv:1509.03512

# Microscopic picture of friction induced shear thickening

Frictionless granular media shear thin
Frictional granular media shear thicken

dense suspensions: frictional contact forces and viscous drag

$\sigma = \eta\dot{\gamma}$

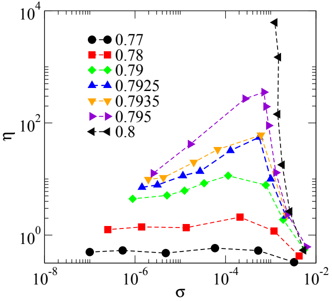


Growing length scale in shear thickening regime

C. Heussinger PRE 2013

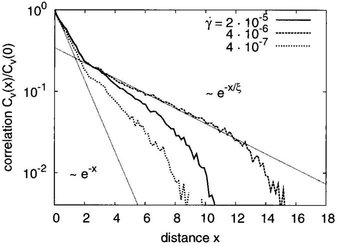


FIG. 4. Velocity correlation function $C_v(x) = \langle v_y(x)v_y(0)\rangle$ for different strain rates and $\phi = 0.7935$.

2 particles in contact:
frictional forces reduce relative motion at the contact point:

$$\boxed{g = v_1^t - v_2^t + \frac{1}{2}(d_1\omega_1 + d_2\omega_2) \to 0}$$

2 extreme cases:

rotations adapt without generating relative translational motion

$$\boxed{v_1^t \sim v_2^t; \quad d_1\omega_1 \sim -d_2\omega_2}$$

exchange of translational and rotational velocities such that

$$\boxed{v \sim d\omega}$$

extend 2-particle picture to patch of size $\xi$

ball bearing state with no relative slip and weak shear resistance

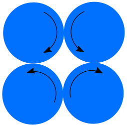

Aström et al. PRL **84**, 638 (2000)
Alonso-Marroquin et al. PRE **74**, 031306 (2006)
Tordesillas et al. PRE **81**, 011302 (2010)
PRE **86**, 011306 (2012)

packing with highest density: all particles in frustrated loops

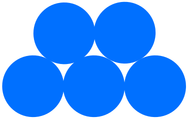

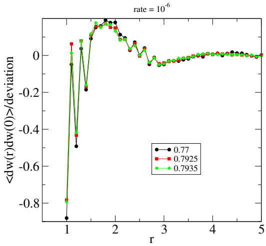


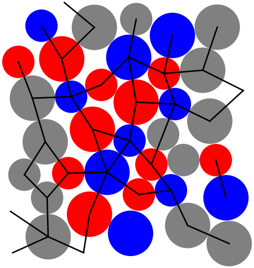

clockwise: red
anti-clockwise: blue

mosaique structure: solid like patches coexisting with clusters of strongly rotating particles

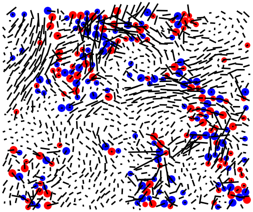

lines: nonaffine velocities; only large $\omega$ are shown

see also Henkes et al.
$\rightarrow$ rigidity percolation

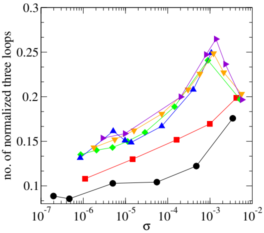


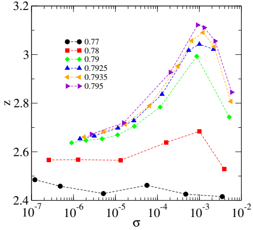


strongly increasing number of 3-loops in the ST regime; solidlike vortices

# Conclusions III

- re-entrant flow, nonzero stress critical point
- van der Waals like phenomenology
- spatio-temporal chaos besides stationary flow and jamming
- observable only for sufficiently large system size
- complex frequency dependent spectra and spatial correlations on scales of system size
- Hydrodynamic model: coupled dynamics of stress and microstructure
- stability analysis: time dependent states
- microstructure $\rightarrow \dot{\gamma}(\sigma) = a\sigma^{1/2} - b\sigma + c\sigma^2$
- microscopic picture: mosaique structure of solid like (frustrated) patches and clusters of strongly rotating particles

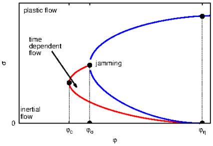


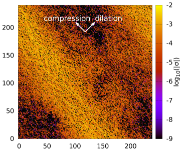


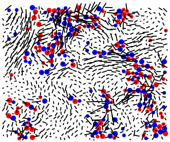

# Thanks to:

Claus Heussinger
(Emmy-Noether)

Matthias Grob
(PhD)

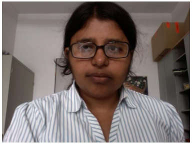

Moumita Maiti
(Postdoc)

Florian Spreckelsen
(Master thesis)